Chemistry–A European Journal
Research Article
doi.org/10.1002/chem.202203860
Chemistry Europe
European Chemical Societies Publishing
www.chemeurj.org

Introducing Aliphatic Fluoropeptides: Perspectives on Folding Properties, Membrane Partition and Proteolytic Stability

Thomas Hohmann[+],[a] Suvrat Chowdhary[+],[a] Kenichi Ataka,[b] Jasmin Er,[a] Gesa Heather Dreyhsig,[a] Joachim Heberle,[b] and Beate Koksch*[a]

Abstract: A de novo designed class of peptide-based fluoropolymers composed of fluorinated aliphatic amino acids as main components is reported. Structural characterization provided insights into fluorine-induced alterations on β-strand to α-helix transition upon an increase in SDS content and revealed the unique formation of PPII structures for trifluorinated fluoropeptides. A combination of circular dichroism, fluorescence-based leaking assays and surface enhanced infrared absorption spectroscopy served to examine the insertion and folding processes into unilamellar vesicles. While partitioning into lipid bilayers, the degree of fluorination conducts a decrease in α-helical content. Furthermore, this study comprises a report on the proteolytic stability of peptides exclusively built up by fluorinated amino acids and proved all sequences to be enzymatically degradable despite the degree of fluorination. Herein presented fluoropeptides as well as the distinctive properties of these artificial and polyfluorinated foldamers with enzyme-degradable features will play a crucial role in the future development of fluorinated peptide-based biomaterials.

Introduction

The introduction of fluorine into bioactive compounds as well as the utilization of fluorocarbon-based polymers attract growing interest in biochemical and pharmaceutical research.[1] Several reports have shown that selective fluorination often can enhance hydrophobic properties and biological activity.[2] It is not surprising that, presently, about 20–25% of commercially available pharmaceuticals do contain fluorinated residues, and perfluorocarbons (PFCs) are widely studied as fluorous tags in the context of gene, protein, and peptide delivery in vitro and in vivo.[3] In general, PFCs are both hydrophobic and lipophobic which ensures superior membrane permeability as well as a promising potential for mediating drug delivery and cell internalization for pharmaceutical applications.[4] For example, conjugation or co-assembly of fluoroalkanes with cargo peptides and proteins was reported to significantly enhance intracellular uptake.[5] A notable drawback of perfluorinated compounds, however, comprises their biological inertness prohibiting biodegradation by digestive enzymes, microbes, and metabolic processes. As a result, PFCs have shown to be very persistent in the environment and can undergo bioaccumulation and biomagnification.[6] Consequently, the development of biodegradable fluoropolymers is of paramount importance to design next-generation biomaterials.[3b]

Incorporation of fluorinated amino acids into peptide & proteins has gained significant relevance in biosciences as it imparts unique biophysical features, like an enhancement in thermal and chemical stability or modulation of folding properties.[7] Depending on the degree of fluorination and side chain pattern, these synthetic building blocks can be used to fine-tune peptide secondary structure formation and bioactivity.[8] Replacing a hydrophobic amino acid with its fluorinated counterpart was reported to facilitate peptide self-assembly in membrane environments, mimicking the properties of fluoroalkyl tags discussed before. For example, Godbout et al. reported a fluorinated 21-residue peptide and showed that fluorous interactions, derived from six residues of (2*S*)-4,4,4-trifluoroethylglycine (TfeGly), drive the assembly into helical superstructures. These biomaterials functioned for the generation of artificial ion channels in lipid bilayers.[9] Furthermore, Naarmann et al. and Bilgiçer et al. described the incorporation of hexafluoroleucine (up to seven residues) into a coiled-coil motif to efficiently drive the formation of defined helical bundles in lipid bilayers and SDS micelles.[10] Finally, fluorine can be a powerful tool to study the interaction of membrane-active peptides with lipids using ^{19}F NMR and has an essential significance for in vivo ^{19}F magnetic resonance imaging.[1c,11]

[a] *T. Hohmann,[+] S. Chowdhary,[+] J. Er, G. H. Dreyhsig, Prof. Dr. B. Koksch*
Institute of Chemistry and Biochemistry
Freie Universität Berlin
Arnimallee 20, 14195 Berlin (Germany)
E-mail: beate.koksch@fu-berlin.de

[b] *Dr. K. Ataka, Prof. Dr. J. Heberle*
Department of Physics
Freie Universität Berlin
Arnimallee 14, 14195 Berlin (Germany)

[+] *Authors contributed equally.*

Supporting information for this article is available on the WWW under https://doi.org/10.1002/chem.202203860

The Koksch laboratory has recently established the access to a variety of aliphatic fluorinated amino acids in gram scale, enabling the fabrication of synthetic peptides consisting of multiple of these building blocks.[12] One of our recent works demonstrated the impact of fluorine-specific interactions to be controlled by the degree of side chain fluorination as well as the overall proportion of fluorinated building blocks.[13] Our ultimate goal, therefore, is the systematic de novo design of peptide-based fluoropolymers with distinct fluorine-driven folding & assembly properties while the peptide scaffold is predestined to maintain biodegradability and biocompatibility.

In this study, we introduce the first generation of fluorine-rich peptide oligomers with diverse chain lengths and degrees of side chain fluorination by the consecutive coupling of either 2-aminobutyric acid **1a** or its fluorinated analogs (2S)-4-monofluoroethylglycine (MfeGly) **1b**, (2S)-4,4-difluoroethylglycine (DfeGly) **1c** or (2S)-4,4,4-trifluoroethylglycine (TfeGly) **1d**. These fluoropeptides were studied with respect to a wide range of biophysical parameters such as hydrophobicity, secondary structure formation, but also the allocation and conformation within interfacial layers of artificial membranes using a combination of CD spectroscopy, 6-FAM leaking assays and surface enhance infrared absorption spectroscopy (SEIRAS)[14]. Furthermore, we present investigations on the proteolytic stability of these fluoropeptides with an exceptional fluorine content (up to 28.5%). To our own surprise, obtained experimental data revealed these fluoropeptides to be enzymatically degradable, regardless of the degree of side chain fluorination. Hence, this data set provides insights into an unexplored class of foldamers constituted at the multidisciplinary interface of peptide science and fluorine chemistry.

Results and Discussion

Peptide design & synthesis

With the aim of systematically studying the impact of fluorination degree of the single building blocks on the overall hydrophobicity, folding and proteolytic stability, the corresponding sequences were constructed from amino acids with different amounts of fluorine. For this purpose, we used 2-aminobutyric acid **1a** and its fluorinated analogs MfeGly **1b**, DfeGly **1c**, and TfeGly **1d** (Figure 1a).

A solubility tag consisting of three or four lysine residues was introduced at the C-terminus of each peptide to facilitate solubility in physiological conditions. The concentration determinations by UV absorbance were achieved by the incorporation of a tyrosine residue. Finally, we included a glycine residue to separate the fluoropeptide sequence from the solubility tag. The N-terminus of the peptides was acetylated. In addition to the degree of fluorination, we examined the influence of the length of the fluoropeptide fragment on above-discussed properties of the respective peptides. Three different lengths, 10, 13, and 15, were selected for this purpose, with three lysine residues (as solubility tag) added to the decamers and four lysines attached to the longer sequences 13 and 15. Hence, a total of twelve peptides was to be synthesized: $X_{10}GY(K)_3$ (X=A, Abu **2a**; M, MfeGly **2b**; D, DfeGly **2c**; T, TfeGly **2d**), $X_{13}KY(K)_4$ (X=A, Abu **3a**; M, MfeGly **3b**; D, DfeGly **3c**; T, TfeGly **3d**), and $X_{15}GY(K)_4$ (X=A, Abu **4a**; M, MfeGly **4b**; D, DfeGly **4c**; T, TfeGly **4d**) (Figure 1a). All peptides studied in this work were synthesized using microwave-assisted solid-phase peptide synthesis (SPPS). By using optimized coupling conditions recently published by Leppkes et al.,[15] all fluorinated amino acids could be incorporated with using only 1.5 equivalents of fluorinated species. *N*,*N*′-Diisopropylcarbodiimide (DIC) and ethyl cyanohydroxyiminoacetate (oxyma) were used as the coupling reagents (Figure 1b). After full cleavage from the resin, the peptides were purified by RP-HPLC (Figure 1c).

Looking at the yields of the peptides, it quickly emerges that the trifluorinated sequences are by far the most difficult to synthesize (Figure 1d). The yields of $TfeGly_{10}GY(K)_3$ **2d** and $TfeGly_{13}GY(K)_4$ **3d** are among the lowest in the series. $TfeGly_{15}GY(K)_4$ **4d** was only synthesized in traces and could not be isolated. The highest yield was achieved with the non-fluorinated decamer $Abu_{10}GY(K)_3$ **2a**. In general, longer homo-oligopeptide sequences are, as expected, more difficult to generate, which can be explained by the increased tendency to aggregate.[16] Therefore, structural investigations were carried out with eleven isolated peptides.

Hydrophobicity of fluoropeptides

Since PFCs can be used as efficient tools to facilitate the uptake by cell membranes, we were especially eager to study the properties of fluoropeptides not only in aqueous but also in lipophilic environments. We assumed that hydrophobicity of the corresponding peptide sequences should be a driving force behind the interactions with membrane models. To quantify the corresponding individual lipophilicity values for each peptide studied in this work, we adapted an HPLC-based assay that was used to estimate the log P values of small organic molecules. A library of tri-, tetra- and pentameric peptides with known log P values was used to determine the unknown log *P* values for the peptides of interest using their retention times on a reversed-phase C18 column (Supporting Information). In Figure 2, the corresponding data are presented. The comparison to the hydrophobicity of the Fmoc-protected amino acids (Supporting Information, Figure S33), which were previously determined and published in our group, shows that the log P values of $X_{10}GY(K)_3$ peptides (X = Abu **2a**, MfeGly **2b**, DfeGly **2c**, TfeGly **2d**) have the same tendencies.

Monofluorination lowers the hydrophobicity compared to the non-fluorinated variant while the di-, and trifluorination increase the log P values. The elevation of polarity by monofluorination was expected and has already been discussed extensively in the literature.[8] This finding can be readily explained by the fluorine-induced dipole moment within the aliphatic side chain. Furthermore, it is characteristic how considerably the trifluorination increases the hydrophobicity of the peptide: the log P of the five residues shorter $TfeGly_{10}GY(K)_3$ **2d** peptide (3.16) is nearly the same as the value of the

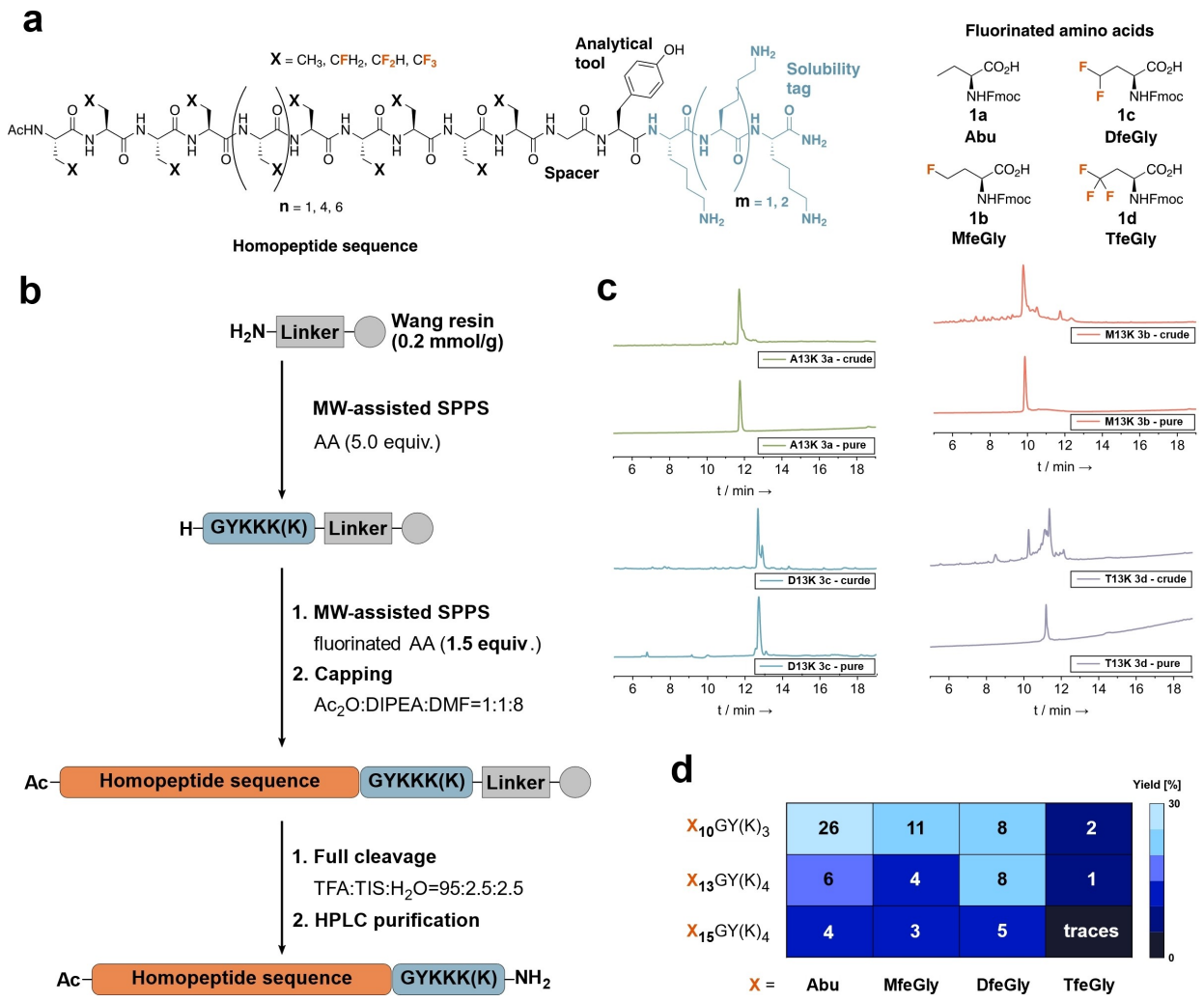

Figure 1. a. The design of fluoropeptides and the structure of fluorinated amino acids that were used as building blocks for the corresponding homooligopeptide sequences; **b**. Microwave-assisted SPPS of fluorinated peptides. Fluorinated amino acids were incorporated with only 1.5 equiv; **c**. HPLC chromatograms of crude and purified $X_{10}GY(K)_3$ **3a**–**d** peptides; **d**. Heat map diagram that demonstrates the dependence of the isolated yields on the length of the homooligopeptide sequence and the degree of fluorination.

$DfeGly_{15}GY(K)_4$ **4c** peptide (3.20). What is additionally striking is the change in polarity between the non-fluorinated and difluorinated peptides. $DfeGly_{10}GY(K)_3$ **2c** peptide is more hydrophobic then the corresponding non-fluorinated peptide with the same length. However, a different picture emerges for longer sequences. DfeGly peptides are less hydrophobic as their non-fluorinated variants with the difference in the log P values also rising with increasing chain length. This indicates a cooperative effect in the case of difluorinated peptides.

Structural investigations in SDS

We studied the structural properties of the de novo designed fluoropeptides using sodium dodecyl sulfate (SDS) micelles as a simple membrane model. Hence, we measured circular dichroism (CD) in phosphate buffer at pH 7.4 at different SDS concentrations (0, 2.5, 5, 10, 20, 40 mM). In Figure 3, the corresponding results are summarized.

Depending on the fluorination degree of the side chain, different trends were observed. Non-fluorinated Abu peptides formed a β-strand structure in water indicated by a minimum at 218 nm and a maximum at 198 nm in the CD spectra. By increasing the SDS content, the peptide conformation changed to an α-helical structure evident from the acquired minimum at 208 nm. An isodichroic point near 200 nm could be observed during this transition indicating a two-state equilibrium for all three Abu peptides. Furthermore, a dual wavelength parametric test can be carried out. Hereby, a constant slope between CD ellipticities at two different wavelengths is a great indicator for a two-state transition.[17] For all Abu peptides, good correlation of SDS concentration-dependent θ_{208} vs. θ_{222} values could be observed (Supporting Information, Figures S35–37). As expected, the α-helix conformation was more stable with longer peptide sequences. Thus, for the transition from the β-strand to

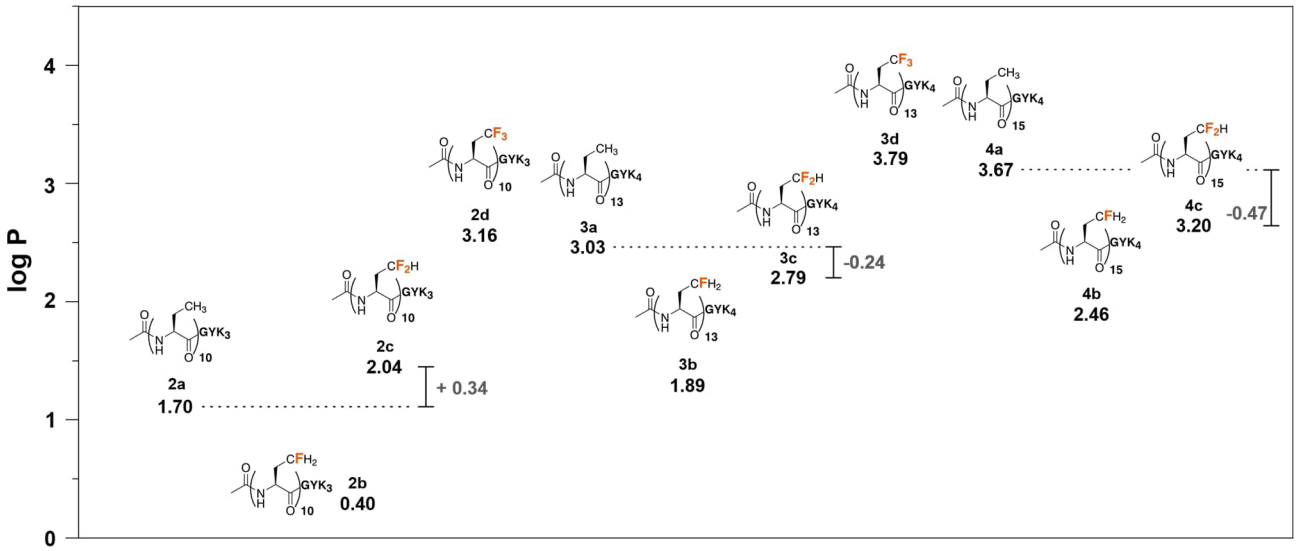

Figure 2. Determined log P values of the fluorinated peptides. The relative increase in polarity of the difluorinated peptides with respect to the nonfluorinated analogues was highlighted.

the α-helix in the case of $Abu_{15}GY(K)_4$ **4a**, an SDS concentration of 2.5 mM was already sufficient. Similar transition was observed for the mono- and difluorinated peptides. An important distinction, compared to the non-fluorinated compounds, is both the stronger influence of the length of the corresponding fluoropeptide sequence, and the minimal amount of SDS required for the stabilization of the α-helix. This trend can be described very well in the case of DfeGly peptides. $DfeGly_{10}GY(K)_3$ **2c** peptide forms a β-strand structure in water. With increasing amount of SDS, the signal diminishes significantly indicating an unordered structure and peptide precipitation at high SDS concentrations.

In the case of $DfeGly_{13}GY(K)_4$ **3c** and $DfeGly_{15}GY(K)_4$ **4c**, a β-strand to α-helix transition was observed as well. Nevertheless, especially for $DfeGly_{13}GY(K)_4$ **3c**, a concentration of 40 mM was required to see a distinct band in the 208 nm region. Analogous conclusions can be drawn for the monofluorinated peptides. A longer sequence or higher SDS amount is needed for the stabilization of the α-helical conformation in a SDS environment. For $DfeGly_{15}GY(K)_4$ **4c** and apart from one exception for $DfeGly_{13}GY(K)_4$ **3c**, an isodichroic point near 200 nm could be detected indicating a two-state transition. Dual wavelength parametric test supports a two-state model, with larger deviations in the slope of the θ_{208} vs. θ_{222} correlation seen in the case of $DfeGly_{13}GY(K)_4$ **3c** (Supporting Information, Figures S38, 39). This was not observed in the case of MfeGly peptides, suggesting a more complex composition of multiple conformations, besides α-helix and β-strand structures.

At this point, it should be mentioned that despite the Lys-tag, the solubility of the peptides in the aqueous medium was severely limited. Therefore, the CD studies described in this work were performed at concentrations between 25 and 50 μM. Apart from $DfeGly_{10}GY(K)_3$ **2c**, no peptide precipitation was observed upon increasing the SDS concentration.

Subsequently, we wanted to use the obtained log P values to explain the tendency to form α-helical structure in the presence of SDS micelles for Abu, MfeGly and DfeGly peptides. The Figure S34 shows the normalized molar ellipticity at 208 nm of the corresponding peptides at different SDS concentrations, which is characteristic for the transition from a β-strand structure to an α-helix. The presented trends show that four of the peptides with the highest log P values also exhibit the strongest α-helical structure formation. An exception is $Abu_{10}GY(K)_3$ **2a**, which, despite its comparatively low hydrophobicity, displays a strong tendency to α-helix formation in the presence of SDS. In addition to hydrophobicity, the length of the peptides seems to be a crucial factor for the stabilization of the α-helical structure in a membrane environment. The $X_{10}GY(K)_3$ **2a-d** and $X_{13}GY(K)_4$ **3a-d** peptides of mono and difluorinated amino acids exhibit the lowest helical content in the vicinity of micelles. In conclusion, mono- and difluorination tend to disrupt the α-helix formation in a hydrophobic environment, which is somewhat consistent with the increase in polarity relative to the non-fluorinated sequences.

Quite unexpectedly, the trifluorinated peptides revealed a completely different picture. Neither an α-helix nor a β-strand conformation could be identified. For $TfeGly_{10}GYK_3$ **2d**, a minimum at 214 nm was observed, which is significantly blue shifted from a minimum at 218 nm that corresponds to a β-strand structure. Additionally, a band at 198 nm was not observed making a β-strand conformation highly unlikely. The CD spectrum of $TfeGly_{13}GY(K)_4$ **3d** shows a minimum at 196 nm and a broad positive band in the 220 nm region. Since the later CD spectrum is somewhat more distinct, we will start our discussion with the structural properties of $TfeGly_{13}GY(K)_4$ **3d**.

Both bands are signatures of a polyproline type II (PPII) helix.[18] Poly(l-prolines), their derivatives, poly(L-lysine) and comparable peptides are known to adapt a PPII conformation[19], an extended left-handed helix (3.1 Å per

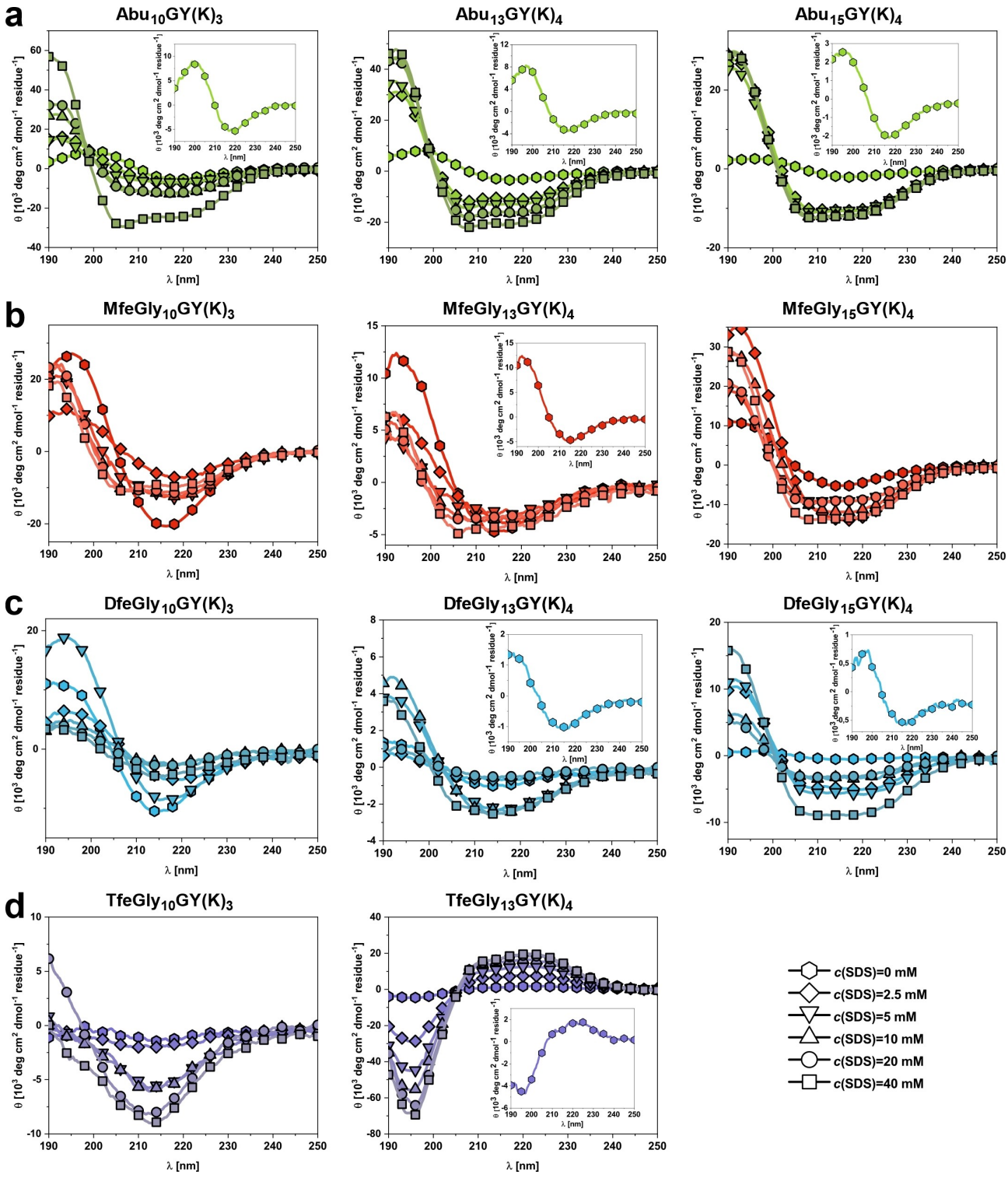

Figure 3. CD spectra of (fluorinated) peptides (25 μM) in aqueous solution (phosphate buffer, 10 mM, pH = 7.4) and in the presence of SDS (2.5, 5, 10, 20, 40 mM); **a**. CD spectra of Abu oligomers; **b**. CD spectra of MfeGly oligomers; **c**. CD spectra of DfeGly oligomers; **d**. CD spectra of TfeGly oligomers. The insets show the zoomed-in spectra at a SDS concentration of 0 mM.

residue) and defined by backbone dihedral angles ϕ, ψ of -75° and +145° (CD spectrum: minimum at 206 nm; maximum at 225 nm).

In the case of $TfeGly_{13}GY(K)_4$ **3 d**, the intensity of both bands increases drastically with the amount of SDS indicating a stabilization of a PPII helix in a hydrophobic environment (additional discussion corresponding the PPII structure is placed

in the Supporting Information). This was rather surprising, since the hydrogen bond network between backbone and water molecules is generally considered to be the greatest stabilizing factor for the PPII conformation.[18a,d,20] Nevertheless, the Budisa research group could already demonstrate based on their work on octahydroindole-2-carboxylic acid oligomers that a PPII conformation can also be formed in a transmembrane environment.[21] In this context, it should be mentioned that these are highly rigid structures which are locked in a PPII conformation. Flexible peptides, analogous to TfeGly oligomers, that can form a PPII helix in a membrane environment are, to the best of our knowledge, unknown. In addition to the backbone solvation, other factors, such as side chain-side chain interactions or side chain conformational entropy, were discussed as possible ways to stabilize a PPII conformation.[18a,22] Particularly in the case of poly(l-lysine) peptides, the repulsion between positive charges of the corresponding side chains was discussed as an important factor for the formation of a PPII structure forcing the peptide chain into an extended conformation.[22–23] Similar considerations could also apply to TfeGly oligomers. Recently, we reported a structural study discussing an alternating peptide structure consisting of TfeGly and lysine residues. Molecular dynamics simulations showed that the most stable structural state of CF_3 groups decline spatial proximity to each other.[13] Here we observe something comparable: In contrast to Abu, MfeGly, and DfeGly oligomers, an α-helical structure is not formed in the presence of SDS. In case of TfeGly-derived fluoropeptides, the CF_3 residues with *i, i +4* spacing turn out to be unfavorable and, thus adopt an extended PPII conformation. Furthermore, an isodichroic point near 206 nm was detected. Additionally, an excellent correlation with a constant slope was observed for the wavelengths at 196 and 221 nm (Supporting Information, Figure S40). Both factors highly support a two-state transition model for the $TfeGly_{13}GY(K)_4$ **3 d** peptide in the presence of SDS. It should be mentioned that in the case of $TfeGly_{13}GY(K)_4$ **3 d**, the band at 220 nm appears very broad compared to poly(l-lysine). This might be due to the influence of tyrosine on the one hand, but on the other hand it could also involve secondary solvent effects. Kubyshkin et al. showed in their work that especially the positive band of the PPII conformation can be very strongly influenced by the environment.[24]

To get a better insight into the structural properties of $TfeGly_{10}GY(K)_3$ **2 d**, we explored the influence of multiple solvents with varying polarity on its structure (Supporting Information, Figure S41). Octan-1-ol simulates an strong hydrophobic environment. Consistent with the results of $TfeGly_{13}GY(K)_4$ **3 d**, $TfeGly_{10}GY(K)_3$ **2 d** adopts a PPII conformation as well. Moreover, it seems that the $TfeGly_{10}GY(K)_3$ **2 d** peptide adopts a PPII conformation in membrane-like environment while in a more polar environment at least one further conformation may be present. In hexafluoroisopropanol (HF*i*P), representing a fluorous-polar solvent, the CD spectrum showed a minimum below 200 nm, but a positive band at a wavelength above 210 nm was absent. This finding could be indicative of a higher random coil fraction[25]. Consequently, experimental data confirms the PPII structure in the case of TfeGly oligomers more likely to be supported by a hydrophobic environment. Subsequently, the structure of $TfeGly_{10}GY(K)_3$ **2 d** in phosphate buffer was examined more closely (Supporting Information, Figure S42). At a 25 mM concentration, the spectrum is reminiscent of a random coil structure. The spectrum at 50 mM showed a minimum at 214 nm, as mentioned earlier. The inlet in Supporting Information shows divergence in the CD spectra of $TfeGly_{10}GY(K)_3$ **2 d** at 25 μM and at 50 μM in phosphate buffer. The corresponding spectrum resembles a β-strand type CD spectra.[20a,26] In general, PPII helix is mostly in a multi-conformational equilibrium with β-strand, β-turn and unordered structures, which can be explained by the great similarities in the corresponding backbone dihedral angles.[18d] Therefore, it seems only consistent and completes the picture that $TfeGly_{10}GY(K)_3$ **2 d** forms multiple conformations, like β-strand, besides the PPII helix. Furthermore, the comparison between $TfeGly_{10}GY(K)_3$ **2 d** and $TfeGly_{13}GY(K)_4$ **3 d** shows that the longer peptide seems to be better accommodated in a more hydrophobic environment. If $TfeGly_{10}GY(K)_3$ **2 d** shows a PPII helix in a strictly hydrophobic medium, as a consequence, it intercalates less strongly with the micelles in the presence of SDS, resulting in a CD spectrum with a higher β-strand fraction.

Structural studies in presence of POPC/POPG

To further deepen our insights into the structural properties of fluoropeptides, especially focusing on their interactions with biomembrane models, CD measurements were carried out in the presence of unilamellar vesicles. The corresponding liposomes were composed of 1-palmitoyl-2-oleoyl-glycero-3-phosphocholine (POPC) and 1-palmitoyl-2-oleoyl-sn-glycero-3-(phosphor-rac-(1-glycerol)) (POPG) lipids (1:1 ratio). Negatively charged POPG was used to facilitate the peptide-liposome interactions. Figure 4a summarizes the CD spectra of all eleven peptides in the presence of POPC/POPG. It must be noted that the measurements were made at a much smaller liposome/peptide ratio of 150:1 compared to the studies with SDS (SDS/peptide = 1600:1, for 40 mM SDS concentration). CD measurements at higher liposome concentrations and at wavelengths below 200 nm were not possible due to the absorbance properties of the liposome suspension. Overall, it can be stated that almost identical trends, compared to the SDS studies, were observed. Again, the most pronounced α-helical structures were formed by $Abu_{13}GY(K)_4$ **3 a**, $Abu_{15}GY(K)_4$ **4 a** and $DfeGly_{15}GY(K)_4$ **4 c**. For other difluorinated peptides and especially for the monofluorinated analogs, CD spectra with higher β-strand content were detected. In synergy to prior data, the length of the peptides and their hydrophobicity are the two decisive factors for the formation of a helical structure in a hydrophobic environment, with monofluorination reducing the stability of that conformation. Both TfeGly peptides adopt a different structure under these conditions. A maxima at wavelengths above 210 nm could be observed indicating the formation of PPII structures. Interestingly, in the case of liposomes, $TfeGly_{10}GY(K)_3$ **2 d** adopts this conformation as well. In a time-dependent manner, comparable to the SDS CD

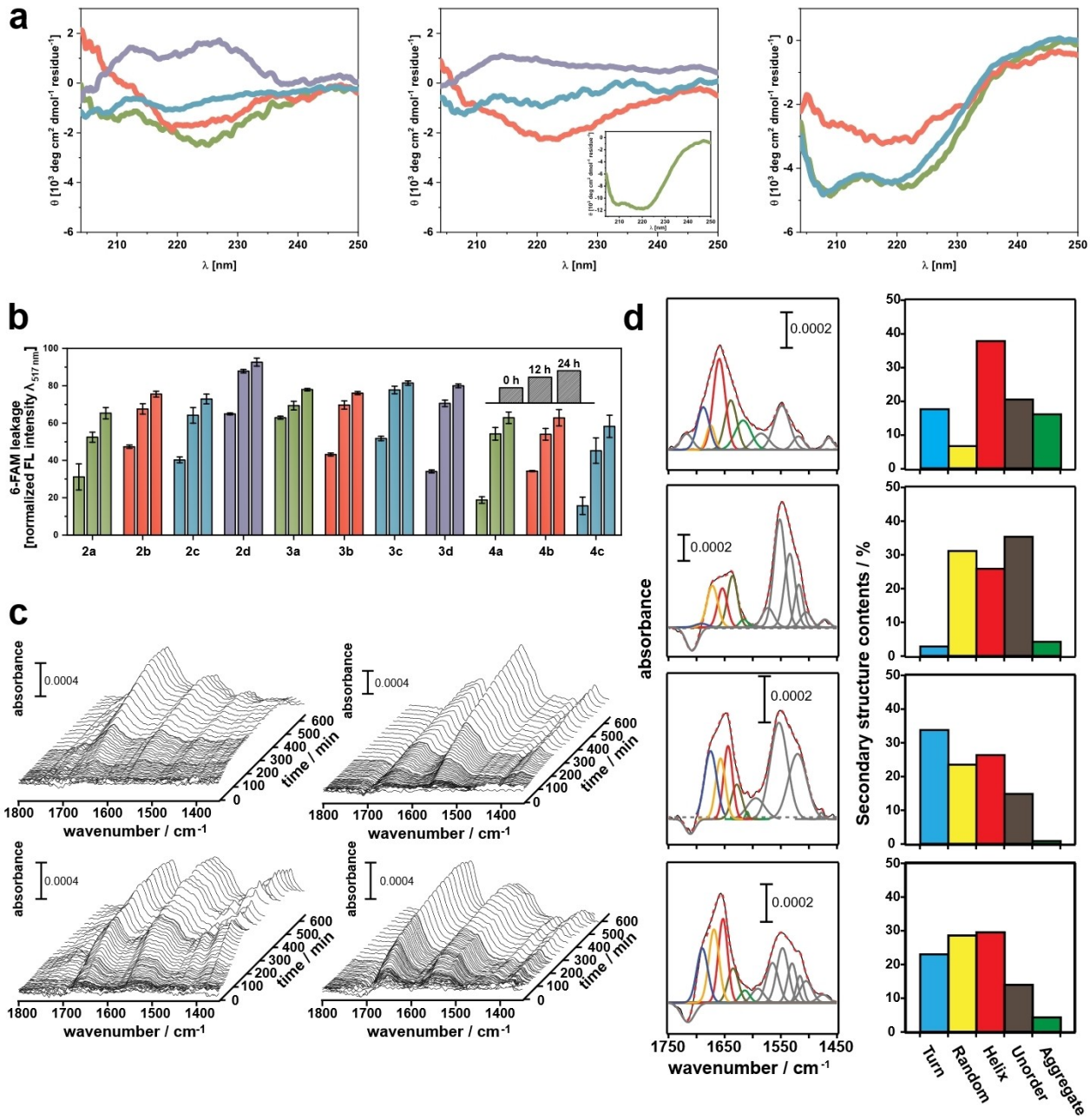

Figure 4. a. Circular dichroism spectra of fluorinated peptides (25 μM) in the presence of POPC:POPG = 1 : 1 (liposome:peptide = 150 : 1) in phosphate buffer (10 mM, pH = 7.4) [left: $X_{10}GY(K)_3$ / center: $X_{13}GY(K)_4$ / right: $X_{15}GY(K)_4$]; **b**. Monitored leakage of the 6-FAM dye (ratio: 1 : 100 peptide:lipid); **c**. In-situ SEIRA spectra of the adsorption process of $X_{13}GY(K)_4$ **3 a–d** peptides on the POPG/POPC lipid bilayer.; **d**. Peak fittings of the amide band of the fluorinated peptides adsorbed on the lipid (**left**) and contents of the secondary structure components (**right**) of $Abu_{13}GY(K)_4$ **3 a** (**first row**), $MfeGly_{13}GY(K)_4$ **3 b** (**second row**), $DfeGly_{13}GY(K)_4$ **3 c** (**third row**), and $TfeGly_{13}GY(K)_4$ (**fourth row**).

spectra, a minimum at 214 nm is formed and the maximum disappears (Supporting Information, Figure S44). This contradicts the hypothesis that a PPII conformation occurs almost exclusively in a hydrophobic environment as $TfeGly_{10}GY(K)_3$ **2 d** seems rather to exhibit several conformations (PPII, β-strand) in the presence of micelles as well as in the presence of liposomes. For $TfeGly_{13}GY(K)_4$ **3 d** peptide, no time-dependent structural changes were observed.

The disruptive interactions of fluoropeptides with liposome vesicles was studied by a fluorescence-based leakage assay using 6-carboxyfluorescein (6-FAM) as a fluorescence dye. For all eleven peptides an increase in fluorescence could be observed due to an intrusion of peptides into the membrane bilayer (Figure 4b). What was already indicated by CD data was also demonstrated by the leakage assay: the penetration of fluoropeptides into the liposomes is a slow process, with fluorescence saturation occurring after approximately 10 h. To

study the structure formation in the course of peptide-membrane interactions, we subsequently carried out infrared spectroscopy experiments.

Surface enhance infrared absorption spectroscopy (SEIRAS)

Since conventional FTIR spectroscopy is not sufficiently sensitive to detect the peptide oligomers at the given concentration, we employed Surface-Enhanced Absorption Spectroscopy (SEIRAS).[27] For this purpose, large unilamellar vesicles (LUV) of POPC/POPG (1:1) were casted over the SEIRA active gold film surface to form a solid-supported lipid bilayer. The lipid-modified SEIRA chip was submitted to a PBS buffer and the peptides were subsequently added. The sample SEIRA spectra were simultaneously measured to observe adsorption/folding process of the polypeptides on the solid- supported lipid bilayer.[27] For these studies, the X13 K peptides were selected, since here, both all degrees of fluorination were present and the structural diversity within the series was the most pronounced.

Figure 4c shows SEIRA spectra of each peptide. Three-dimensional presentation of these spectra provides overviews on the adsorption process of the peptides. As the peptides were added, two marker bands appeared at around ~1650 and ~1550 cm^{-1} and increased with time. These bands are assigned to amide I and II vibrational modes of the peptide backbone. Increase of these bands indicates a greater partitioning of peptides on the supported lipid bilayer with time. What was already indicated by CD measurements and fluorescence leakage assay was confirmed by SEIRA measurements: the increasing rate of the amide bands for each peptide is relatively slow, with saturation intensity being reached after 200 to 600 minutes depending on the degree of fluorination. SEIRA spectra at the saturation coverage of each adsorbed peptide illustrated that the spectral features of each peptide are very different to each other (Figure 4d). In the non-fluorinated peptide, $Abu_{13}GY(K)_4$ **3a**, amide I and II appear as broad and symmetrical features peaking at 1659 and 1549 cm^{-1}, respectively. These peak positions are typical of α-helical structure of long-chain peptides or proteins, suggesting that the lipid adsorbed $Abu_{13}GY(K)_4$ **3a** is present as an α-helix. On the other hand, amide bands of the fluorinated peptides **3b-d** show characteristic asymmetrical features different from those of $Abu_{13}GY(K)_4$ **3a**. This is consistent with the obtained CD data *(see above)*, which showed different conformational compositions depending on the degree of fluorination.

Peak fitting of the amide I band was carried out and the integrated peak areas were used to quantify the individual secondary structure components. Details of the peak fittings are described in the Supporting Information, section 3.6. We limited the analysis to five representative structures, namely 'Turn/Bend', 'Random', 'Helix', 'Unordered', and 'β-aggregate/sheet'. Since distinction between β-sheet and β-aggregate is difficult due to overlap of absorption region, the contribution from β-sheet structure is included in 'β-aggregate' structures. The component bands appear in the range of 1675–1695 cm^{-1} (Turn), 1660–1675 cm^{-1} (Random), 1660–1645 cm^{-1}(helix), 1630–1645 cm^{-1} (Unordered), 1610–1630 cm^{-1} (Aggregate), respectively (Figure 4d). For non-fluorinated $Abu_{13}GY(K)_4$ **3a** peptide, the predominant component is a helical structure, which occupies about 40% of the conformational space. This is in agreement with our CD measurements, which showed that Abu oligomers have the highest tendency of all investigated peptides to from α-helical structures. In the case of both $MfeGly_{13}GY(K)_4$ **3b** and $DfeGly_{13}GY(K)_4$ **3c**, the helical fraction decreases significantly (26% for $MfeGly_{13}GY(K)_4$ **3b** and $DfeGly_{13}GY(K)_4$ **3c**). Something similar was also shown by the CD spectra, which indicated a more complex conformational composition with a lower α-helical content in a hydrophobic environment. If the $TfeGly_{13}GY(K)_4$ **3d** is compared with $DfeGly_{13}GY(K)_4$ **3c**, it can be observed that the proportion of bend/turn structures decreases (from 34 to 23%) and slightly increases in the case of the helical structure (26 to 30%). As discussed in detail in the previous sections, no alpha helix was observed during CD experiments with trifluorinated peptides. Unfortunately, the discrimination of different helical structures by IR spectroscopy is difficult. Therefore, we interpret the observed higher content of helical structure, compared to the monofluorinated and difluorinated peptides, as presence of an extended helical conformation.

Truncated fluoropeptides: folding, membrane partition and proteolysis

As discussed before, PFCs hardly degrade under environmental conditions and are often characterized as persistent. Therefore, we raised the question about the proteolytic stability of the fluoropeptides. Preliminary studies showed that fluoropeptides with solely fluorous residues about $n \geq 6$ are insoluble in aqueous conditions. To accomplish efficient proteolysis studies, a sufficient solubility of starting material is required. The $GYK_{3/4}$ tag in above-discussed library would immediately be degraded by the protease and, thus, cannot serve for elucidation of the fluoropeptides' degradability. We, therefore, established a small new library of truncated fluoropeptides (X_4[4]Abz; with X = Abu (Abu_4[4]Abz) **5a**, MfeGly ($MfeGly_4$[4]Abz) **5b**, DfeGly ($DfeGly_4$[4]Abz) **5c** & TfeGly ($TfeGly_4$[4]Abz)) **5d**) which are soluble in given conditions of the peptide digestion assay. On the C-terminus, *para*-aminobenzoic acid [4]Abz was attached for determination of peptide stock concentrations.[28] Acetylation of the N-terminus was omitted to provide a somewhat net charge on this hydrophobic scaffold (Figure 5).

At first, we aimed to explore whether previously described observations on fluorine-directed peptide folding in lipid environments can be also complied to truncated derivatives. CD experiments were done in physiological conditions at 100 μM peptide concentration and varying amounts of SDS (10 mM, 20 mM, 40 mM) as discussed before (Figure 6a). We observed for the labeled tetrapeptides Abu_4[4]Abz **5a** and $DfeGly_4$[4]Abz **5c** a global minimum at 198–200 nm and a shallow minimum at 218 nm. This CD pattern can be interpreted as a mixture of disordered peptide ($\lambda_{min} = 198$ nm) and

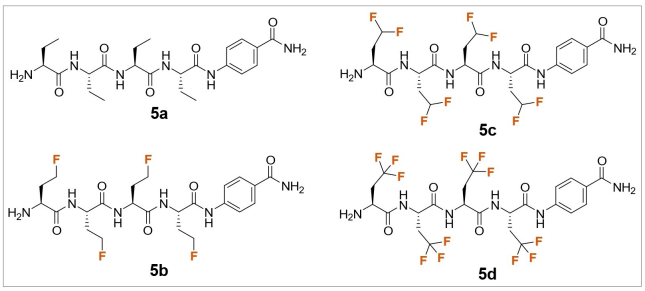

Figure 5. Chemical structures of labeled fluoropeptides (X_4[4]Abz series).

minor amounts of β-strand-like conformations (λ_{min} = 218 nm). This evaluation is in accordance with prior work by Schweitzer-Stenner and co-workers.[29] The latter minimum was not observed for the MfeGly-derived tetrapeptide, indicating a major presence of random coils. The general absence of β-sheet to α-helix transitions as described for the $X_{10}GY(K)_3$, $X_{13}GY(K)_4$ and $X_{15}GY(K)_4$ series can be explained by the short sequence length of the $[X]_4$[4]Abz series and, consequently, a lack of the typical backbone *i*→*i-4* hydrogen bonding pattern as indispensable criterion for α-helical structures.

For $TfeGly_4$[4]Abz **5 d**, however, we determined the typical course of adsorption for β-strands due to the negative band between 218–220 nm and positive band between 195–200 nm. Upon addition of SDS (10 mM–20 mM) the β-strand content increases significantly as observed in the wavelength shift for the negative band to around 215 nm and increased ellipticity at 195 nm. These results are in good agreement with prior reports by Barnham and co-workers about SDS-generated stabilization of Aβ-derived β-sheet conformers.[30] It is most noteworthy that higher amounts of SDS (40 mM) lead to a further shift of the global minimum to about 210 nm, indicating a coexistence of different folding patterns. As discussed before for $TfeGly_{10}GY(K)_3$ **3 d** and $TfeGly_{13}GY(K)_4$ **4 d**, this data set would corroborate our considerations about a multiconformational equilibrium in membrane-like environments. Consequently, the observed blue-shift in the CD spectra can be assigned to a growing content of extended PPII-like conformations caused by side chain – side chain interactions. As reported by Rausch et al., a rising degree of structured peptides through SDS addition can correspond to β-stand driven intercalation into lipid bilayers.[31] In a similar manner, 6-FAM leaking assays with POPC:POPG liposomes revealed all X_4[4]Abz peptides to disrupt artificial lipid bilayers but with superior potency for $TfeGly_4$[4]Abz **5 d** after 24 h (about 67 %) in comparison to **5 a**–**c** (about 35 %) (Figure 6b).

Finally, we studied whether these fluoropeptides can be degraded through digestive enzymes. The incorporation of non-natural amino acids in high proportion is a well-known strategy to alter or even eliminate peptide proteolysis.[32] In the context of side chain fluorinated amino acids, a wide range of studies exist with diverse outcomes of such modifications. Moreover, the enzymatic degradation of peptides consisting mainly of fluorinated amino acids has not been studied yet.[33] In this work, we probed the stability of these fluoropeptides towards peptide digestion by the serine proteases elastase and proteinase k. Both endoproteases possess a particular specificity to cleave the amide bonds of aliphatic amino acids at the P1 position.[34] All X_4[4]Abz peptides were dissolved in physiological buffer supplemented with 25 % DMSO and, after addition of enzyme, the amount of degradation was determined via HPLC analysis. Quite unexpectedly, we observed peptide degradation for all fluoropeptides upon incubation with both enzymes (see Figure 6c (left) and Supporting Information, Figure S49). After 6 h incubation after addition of elastase (Figure 6c (right), black line), we found major proportions of all labeled tetrapeptides to be digested. Remaining amounts of Abu_4[4]Abz **5 a** (4.3 ± 0.1 %), $MfeGly_4$[4]Abz **5 b** (6.6 ± 1.1 %), $DfeGly_4$[4]Abz **5 c** (10.9 ± 3.8 %) and $TfeGly_4$[4]Abz (19.3 ± 4.0 %) **5 d** appoint a synergy between the growing degree of fluorination and enhanced proteolytic stability with up to 4.4-fold improved rates upon CH_3 (Abu) to CF_3 (TfeGly) substitution. Nevertheless, these astonishing results display an overall accommodation of the fluoropeptides within the enzymes active site. Real-time monitoring of peptide digestion by proteinase k (Figure 6c (right), red line) validated the enzymatic degradability properties of all fluoropeptides. After 3 h of incubation, $TfeGly_4$[4]Abz **5 d** was mainly degraded by the enzyme but remained in about 3.7-fold increased amounts (9.3 ± 5.0 %) than the Abu-derived tetrapeptide (2.5 ± 0.1 %). Further comparison with leftovers detected for $MfeGly_4$[4]Abz **5 b** (4.4 ± 2.2 %) and $DfeGly_4$[4]Abz **5 c** (2.6 ± 0.3 %) after 3 h highlights the scope of substrate acceptance of both enzymes regardless to the fluorinated side chain pattern. Furthermore, we were engaged to determine predominant cleaving sites via HPLC/MS-assisted analysis (experimental data and discussion are provided in the Supporting Information, Figure S51–S54). It is most noteworthy that the [4]Abz-labeled amino acids Abu, MfeGly, DfeGly or TfeGly were found as remaining digestion fragments for both serine proteases. This confirms a main P1-P1′ scissile bond in which the fluorinated amino acids act as both P1 and P1′ residues, thereby proving susceptibility towards enzymatic degradation in terms of elastase or proteinase K.[35]

Prior studies from our laboratory[33a], but also the research groups of Jakubke[36], Kumar[37] and Marsh[38] came to somewhat contradictory outcomes about the proteolytic stability of peptides when incorporating one or a few fluorinated amino acids. In this study, we investigated the enzymatic degradability of fluoropeptides containing exclusively fluorinated aliphatic amino acids. Experimental evidence obtained in this work let us conclude that these fluoropeptides can be rather considered as biodegradable fluoropolymers than synthetic & persistent PFC-mimicries.

Conclusion

In this work, we present the first series of artificial fluoropeptides ever reported. Depending on the sequence-length and degree of side chain fluorination, we found notable differences in peptide secondary structure formation under membrane-

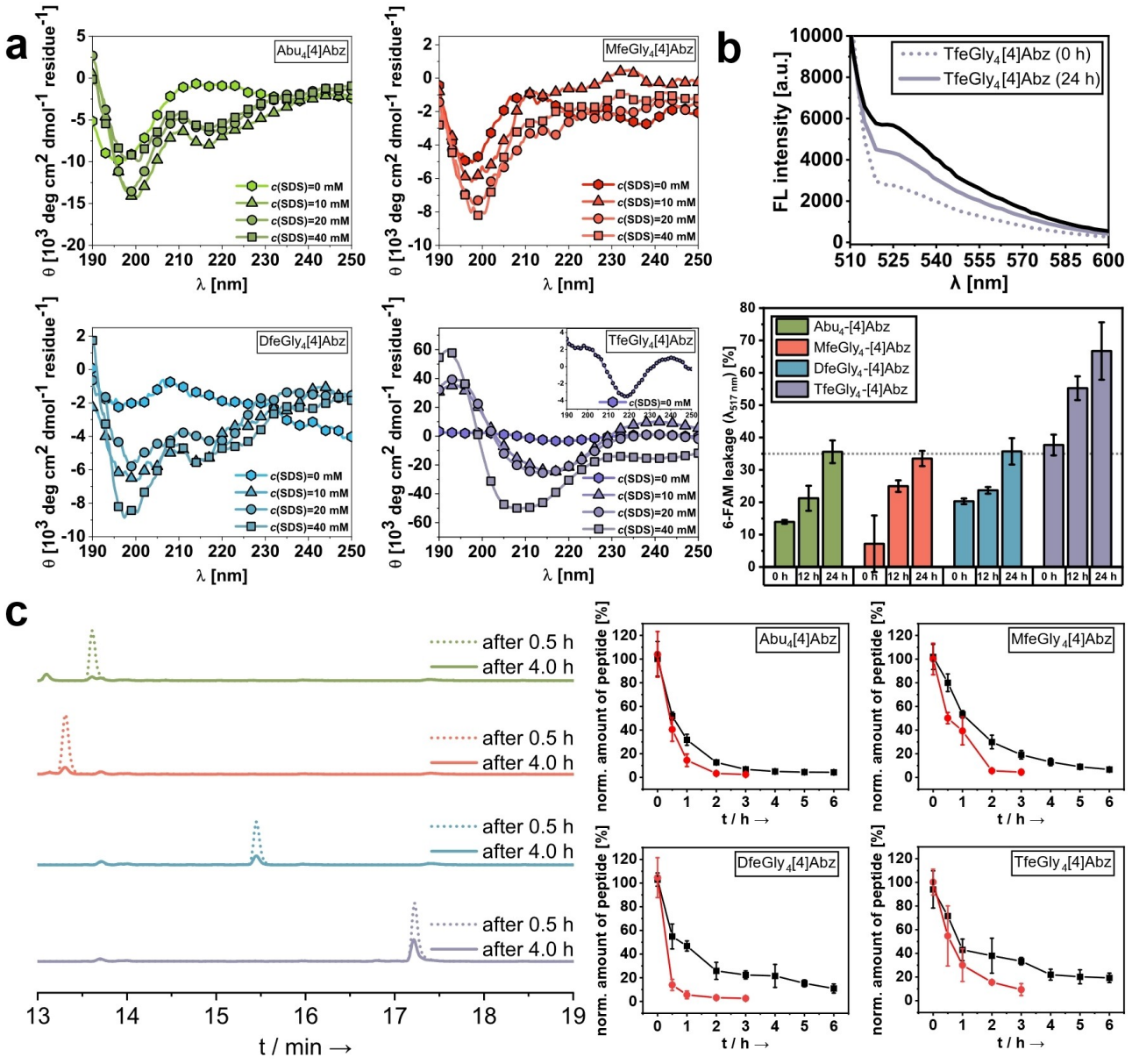

Figure 6. a. CD spectra of truncated fluoropeptides (100 μM) in aqueous solution (phosphate buffer, 10 mM, pH = 7.4) and in the presence of SDS (10, 20, 40 mM). **b**. Monitored increase in FL intensity resulting from dye-release in case of TfeGly$_4$[4]Abz **5 d** (100 μM) during incubation [at the start of experiment (dashed line) and after 24 h incubation (solid line)] in POPC:POPG liposome solution (liposome:peptide = 50:1). The FL intensity derived from the positive control [5% (v/v) Triton X-100 in buffer] is illustrated as black line (**top**). Also, calculated percentages of 6-FAM dye leakage (X$_4$[4]Abz series, liposome: peptide = 50:1) reveal superior membrane-disrupting properties upon CH_3 to CF_3 substitution (**5 d**). Lower degrees of dye leaking resembled by average FL values of about 35% were found similarly for **5 a**, **5 b** and **5 c** and are marked as grey-colored dotted line (**bottom**). **c**. Real-time monitoring of peptide proteolysis for **5 a**–**5 d** by the serine protease elastase depicted after 0.5 h (dashed line) and 4 h (solid line) incubation (colors are the same as presented in **a**. and **b.**) via HPLC analysis (Supporting Information, Table S20) (**left**). Normalized amounts of remaining tetrapeptides (230 μM) determined during enzymatic degradation by elastase (0.91 μM, black line) and proteinase k (0.0091 μM, red line) (**right**).

mimicking environments. A wide range of experimental techniques ranging from CD spectroscopy to SEIRAS, and FL-based leaking assays served to elucidate the intercalation of these fluoropeptides into lipid bilayers and resulting folding patterns. In general, a β-sheet to α-helix transition was observed in most cases series. For the TfeGly-containing fluoropeptides, however, experimental data indicates a unique fluorine-driven formation of PPII structures. Monitoring the partition into POPC:POPG lipid bilayers exposed alterations in structural compositions, like a decrease in α-helical content in response to the total degree of fluorination. Moreover, proteolysis studies of truncated fluoropeptides exclusively built up from fluorinated amino acids revealed an overall degradability. This study lays the foundation for the development of de novo designed foldamers with fluorine-directed folding and membrane-disrupting properties by maintaining biodegradability. We consider this class of peptide-based fluorooligomers to serve as initial templates in the future design of fluorinated

biomaterials as, for example, fluorous tags for biomolecule or drug delivery. Ongoing work focusses on the biocompatibility of these fluoropeptides and will provide further insights into potential biomedical applications.

Experimental Section

General methods: HRMS were determined on an Agilent 6220 ESI-TOF MS instrument (Agilent Technologies, Santa Clara, CA, USA). For analysis, the MassHunter Workstation Software VersionB.02.00 (Agilent Technologies, Santa Clara, CA, USA) was used. All chemicals were purchased from commercial sources (Merck, Sigma-Aldrich, VWR, Fluorochem) and used without further purification. The fluorinated amino acids MfeGly, DfeGly and TfeGly were synthesised according to literature.[12b]

Synthesis and purification of peptides: All fluoropeptides (X_{10}GY-$(K)_3$, X_{13}GY$(K)_4$ and X_{15}GY$(K)_4$ series) were synthesized with a microwave-equipped Liberty Blue™ peptide synthesizer (CEM, Matthews, NC, USA). A Rink Amide ProTide™ resin (CEM, Matthews, NC, USA) was utilized and the synthesis was performed either in 0.05 mmol or 0.1 mmol scale using Oxyma/DIC as activating reagents. Detailed coupling protocols are listed in the Supporting Information. Acetylation was done manually in three batches using acetic anhydride (10% v/v) and DIPEA (10% v/v) in DMF (6 mL). The labeled tetrapeptides X_4[4]Abz were synthesized through standard manual SPPS.

All peptides were cleaved from the resin by treatment with TFA /TIPS/H_2O (90/5/5) [1 mL cleavage cocktail per 50 mg resin] for three hours using sonication at room temperature. Then the resins were washed with TFA and DCM, and excess of solvents were removed by evaporation. Peptides were dried by lyophilization before purification with preparative reversed phase HPLC. Purification of synthesized peptides was performed on a Knauer low-pressure HPLC system (Knauer GmbH, Berlin, Germany) sold by VWR (Darmstadt, Germany), comprising a LaPrep Sigma preparative pump (LP1200), a ternary low-pressure gradient, a dynamic mixing chamber, a 6-port-3-channel injection valve with an automated preparative 10 mL sample loop, a LaPrep Sigma standard 1-channel-UV-detector (LP3101), a flow cell with 0.5 mm thickness and a 16-port LaPrep Sigma fractionation valve (LP2016). A Kinetex RPC18 endcapped (5 μM, 100 Å, 250×21.2 mm, Phenomenex®, USA) HPLC-column was used. A Security Guard™ PREP Cartridge Holder Kit (21.20 mm, ID, Phenomenex®, USA) served as pre-column. As eluents water and ACN, both containing 0.1% (v/v) TFA were applied. HPLC runs were performed with a flow rate of 15.0 mL/min, UV-detection occurred at 220 nm for respective peptides. Data analysis occurred with an EZChrom Elite-Software (Version 3.3.2 SP2, Agilent). After separation, the purity of the collected fractions was determined by analytical HPLC. Analytical HPLC was carried out on a Chromaster 600 bar DAD-System with CSM software or a Hitachi Primaide™ UV-HPLC system (both from VWR/Hitachi, Darmstadt, Germany). A Kinetex® RP-C18 (5 μM, 100 Å, 250 ×4.6 mm, Phenomenex®, USA) column and a SecurityGuard™ Cartridge Kit equipped with a C18 cartridge (4×3.0 mm, Phenomenex®, USA)) as pre-column was used. Otherwise, a Luna® RP-C8 (5 μm, 100 Å, 150×3 mm, Phenomenex®, USA) column was used. As eluents water and ACN, both containing 0.1% (v/v) TFA were applied. A flow rate of 1 mL/min was used and UV-detection occurred at 220 nm or 280 nm for respective peptides. Data analysis was done with EZ Chrom ELITE software (version 3.3.2, Agilent). The resulting pure peptides (>95%) were obtained after lyophilization of the collected fractions. All essential data for the quantification of purified peptides (HPLC chromatograms, HRMS spectra) can be found in the Supporting Information.

CD spectroscopy: Circular dichroism experiments were performed using a Jasco J-810 spectropolarimeter fitted with a recirculating chiller. Data were recorded using 0.1 mm or 0.2 mm Quartz Suprasil® cuvettes (Hellma) equipped with a stopper. Spectra were recorded at 37 °C from 190 to 250 nm at 0.2 nm intervals, 1 nm bandwidth, 4 s response time and a scan speed of 100 nm min^{-1}. Baselines were recorded and were subtracted from the data. Each reported CD value represents the average of minimum three measurements.

Lyophilization: To lyophilize the synthesized peptides a laboratory freeze dryer ALPHA 1–2 LD (Christ Gefriertrocknungsanlagen GmbH, Osterode am Harz, Germany) was used.

Preparation of large unilamellar vesicles (LUV): POPC and POPG were each dissolved in chloroform (1 m). From these stock solutions, POPC and POPG (1:1) were suspended in phosphate buffer (10 mm, pH = 7.4) at a concentration of 3.75 mm. The suspension was submitted to ten freeze and thaw cycles. Subsequently, large unilamellar vesicles (LUVs) were prepared by extrusion across a polycarbonate Nuclepore™ track-etched membrane (0.1 μm pore size, Whatman International Ltd., Kent, United Kingdom) using an Avanti extruder (Avanti Polar Lipids, Birmingham, AL, USA).

6-Carboxyfluorescein [6-FAM] leakage assay: At first, stocks of 1-palmitoyl-2-oleoyl-sn-glycero-3-phosphocholine (POPC) and 1-palmitoyl-2-oleoyl-sn-glycero-3-[phospho-rac-(1-glycerol)] (POPG) were prepared by dissolving the compounds in $CHCl_3$ in a concentration of 10 mg/mL. Aliquots were taken from both stocks and $CHCl_3$ was evaporated. The amount of aliquots corresponded to a liposome solution of POPC/POPG (1:1, each 5 mM [1 mL]). The lipid film was dried *in vacuo* overnight and then dissolved in 50 mM 6-carboxyfluorescein (6-FAM) in 10 mM phosphate buffer, pH 7.4. The pH of this solution was adjusted to pH 7.4 with a 1 N NaOH solution before addition to the lipid film. The suspension was submitted to ten freeze–thaw cycles and then rest for 1 h at rt for equilibration. Untrapped dye was removed by gel filtration on PD-10 desalting columns containing Sephadex G-25. To prepare peptide/lipids sample, aliquots were taken from respective peptide stocks in HFIP and dried under a gentle stream of nitrogen. Then, dried peptide films were dissolved in 25 μL buffer and mixed for 5–10 seconds to obtain a homogeneous mixture. Subsequently, 25 μL of liposome solution were added and the solution was gently mixed for 5 seconds. The final concentrations were: 50 μM (X_{10}GY-$(K)_3$ - X_{13}GY$(K)_4$ - X_{15}GY$(K)_4$ series) or 100 μM peptide (X_4[4]Abz) + 5 mM POPG:POPG (1:1, each 2.5 mM). The leakage of 6-FAM was detected by measuring the fluorescence intensity at 37 °C and an excitation wavelength of 493 nm; fluorescence emission was recorded at 517 nm. 100% dye release was achieved from the liposomes with the addition of 5% (v/v) Triton X-100 in buffer. A negative control was constituted by measuring FL emission of the liposome solution only containing buffer. All samples were transferred on BRAND® microplates (size: 96 wells, color: black; Sigma-Aldrich), sealed to prevent evaporation and placed in an Infinite M Nano$^+$ plate reader (Tecan Deutschland GmbH, Crailsheim, Germany). Fluorescence intensity was followed over 24 h after sample preparation and a fluorescence scan was measured every 30 min.

Estimation of log P values: The estimation of log P values was carried out according a HPLC-based protocol adapted from the O'Hagan working group. A library of short peptides with known log P values was synthesized and analyzed by HPLC. The corresponding retention times were measured using a reversed-phase C18 column. Subsequently, the correlation between known log P values and

retention times was fitted. The obtained linear function was used to estimate the log P values of fluoropeptides from the corresponding measured retention times. A detailed description of the protocol can be found in the Supporting Information.

Peptide digestion assay: For all enzymes, following buffer mixture was used: 50 mM bis-tris propane + 20 mM $CaCl_2$, pH 8 [75%] + DMSO [25%]. All samples were dissolved in buffer (400 μL) and then were gently mixed to obtain a homogeneous solution. Afterwards, 40 μL of an enzyme-solution in buffer (elastase: 10 μM / proteinase k: 0.1 μM) were added and the samples were again gently mixed for 5 seconds. The concentration of each enzyme was adjusted before to obtain well-detectable digestion kinetics. The final concentrations were: 230 μM X_4[4]Abz peptide + 0.91 μM elastase or 0.0091 μM proteinase k. All samples were incubated at 30 °C over a period of 3–6 h. Aliquots of 15 μL were taken at fixed time points and quenched with 90 μL of a solution of 30% AcOH in water containing 130 μM Ac-[4]Abz-Gly-OH as reference. Afterwards, peptide degradation was monitored by HPLC analysis. In all cases, the peaks corresponding to each peptide sample (full-length peptides) and the reference sample were integrated and used to determine the amount of substrate still present in solution. The content of starting material after 5 min was termed as absolute amount for simplicity. For the detection of peptide fragments derived from proteolysis, all samples were prepared accordingly and incubated at 30 °C over a period of 24 h. Afterwards, aliquots of the reaction mixture were monitored by HPLC analysis. To identify the cleaving site of each peptide, each HPLC signal from a digestion fragment cleaved from the full-length peptide was isolated and analyzed by ESI-ToF mass analysis on an Agilent 6220 ESI-ToF-MS spectrometer (Agilent Technologies, Santa Clara, CA, USA).

Surface enhanced infrared absorption spectroscopy (SEIRAS): The required amount of a 1:1 volume ratio of 1-palmitoyl-2-oleoyl-glycero-3-phosphocholine (POPC) and 1-palmitoyl-2-oleoyl-sn-glycero-3-phospho-1'-rac-glycerol (POPG) (Avanti Polar Lipids, Alabama, USA) dissolved in chloroform was placed in a septum capped glass tube and dried under a gentle flow of argon. The dried lipid was resuspended in 10 mM phosphate buffer (pH 6.0). The suspension was freeze-thawed at least 5 times, followed by extrusion with a 100 nm filter to form Large Unilamellar Vesicles (LUV) of POPC/POPG. Then, ~1.2 mg/ml of lipid LUV was casted over the surface of Au film substrate to form a solid-supported lipid layer by spontaneous vesicle fusion. After incubation in the lipid containing solution for overnight (> 12 h), the Au film surface was thoroughly rinsed with Milli-Q water and the buffer solution to remove excess amount of the lipid accumulated over the solid supported lipid bilayer. SEIRAS experiments were conducted as described before.[39] Briefly, Attenuated Total Reflection (ATR) optical configuration was employed with a micro-grooved silicon chip crystal as internal reflection element (IRE, from IRUBIS GmbH, München, Germany). A SEIRA active gold film was formed on reflection surface of IRE by chemical deposition. A background spectrum was taken on the gold surface with presence of the solid supported POPC/POPG bilayer in 200 μL of 10 mM phosphate buffer solution with pH = 7.4 prior to the sample measurement. Then, 200 μL of the peptide samples dissolved in same buffer was added to the solution and sample IR spectra were subsequently measured to monitor the adsorption process on the lipid surface. Finale concentration of each peptide during the adsorption measurement was kept ~25 μg/ml. Baseline of the obtained spectra were corrected at the position of 1800 cm^{-1}, where no absorption from the band relate to the samples occur, to become zero.

Author contributions

T.H. and S.C. developed the overall project, provided fluorinated amino acids, synthesized & purified all fluoropeptides and wrote the manuscript. B.K. provided guidance on data analysis and interpretation. T.H. performed CD studies, structural studies with POPC/POPG liposomes and determination of hydrophobicity. S.C. performed CD studies, leaking & peptide digestion assays. K.A. performed SEIRAS studies and wrote the manuscript. J.E. assisted T.H. in synthesis and analysis. G.H.D. assisted S.C. in synthesis and digestion assays. J.H. provided expertise and feedback.

Acknowledgements

The authors gratefully acknowledge financial support by the Deutsche Forschungsgemeinschaft (DFG) through the collaborative research center CRC-1349 "Fluorine-Specific Interactions" project no. 387284271. T.H. thanks the Studienstiftung des deutschen Volkes for financial support. We thank Dr. Stephan Block, Dr. Katharina G. Hugentobler and Dr. Stephanie Wedepohl for scientific discussions and expertise. We thank Balu and Honey for continuous encouragement and support. We would like to acknowledge the assistance of the Core Facility *BioSupraMol* supported by the DFG. Open Access funding enabled and organized by Projekt DEAL.

Conflicts of interest

There are no conflicts to declare.

Data Availability Statement

The data that support the findings of this study are available in the supplementary material of this article.

Keywords: fluorinated biomaterials · fluoropeptides · fluorous amino acids · foldamers · membrane disruption

[1] a) I. Ojima, *J. Org. Chem.* **2013**, *78*, 6358–6383; b) J. M. Wolfe, C. M. Fadzen, R. L. Holden, M. Yao, G. J. Hanson, B. L. Pentelute, *Angew. Chem. Int. Ed.* **2018**, *57*, 4756–4759; c) E. N. G. Marsh, B. C. Buer, A. Ramamoorthy, *Mol. BioSyst.* **2009**, *5*, 1143–1147.
[2] a) M. P. Krafft, *Adv. Drug Delivery Rev.* **2001**, *47*, 209–228; b) H.-J. Böhm, D. Banner, S. Bendels, M. Kansy, B. Kuhn, K. Müller, U. Obst-Sander, M. Stahl, *ChemBioChem* **2004**, *5*, 637–643.
[3] a) J. Han, A. M. Remete, L. S. Dobson, L. Kiss, K. Izawa, H. Moriwaki, V. A. Soloshonok, D. O'Hagan, *J. Fluorine Chem.* **2020**, *239*, 109639; b) J. Lv, Y. Cheng, *Chem. Soc. Rev.* **2021**, *50*, 5435–5467.
[4] T. Song, Y. Gao, M. Song, J. Qian, H. Zhang, J. Zhou, Y. Ding, *Med. Drug Discovery* **2022**, *14*, 100123.
[5] a) Z. Zhang, W. Shen, J. Ling, Y. Yan, J. Hu, Y. Cheng, *Nat. Commun.* **2018**, *9*, 1377; b) G. Rong, C. Wang, L. Chen, Y. Yan, Y. Cheng, *Sci. Adv.* **2020**, *6*, eaaz1774.
[6] a) T. Stahl, D. Mattern, H. Brunn, *Environ. Sci. Europe* **2011**, *23*, 38; b) V. Ochoa-Herrera, J. A. Field, A. Luna-Velasco, R. Sierra-Alvarez, *Environ. Sci. Process. Impacts* **2016**, *18*, 1236–1246.

[7] C. Jäckel, M. Salwiczek, B. Koksch, *Angew. Chem. Int. Ed.* **2006**, *45*, 4198–4203.
[8] A. A. Berger, J.-S. Völler, N. Budisa, B. Koksch, *Acc. Chem. Res.* **2017**, *50*, 2093–2103.
[9] a) R. Godbout, S. Légaré, M. Auger, C. Carpentier, F. Otis, M. Auger, P. Lagüe, N. Voyer, *PLoS One* **2016**, *11*, e0166587–e0166587; b) M. Auger, T. Lefèvre, F. Otis, N. Voyer, M. Auger, *Pept. Sci.* **2019**, *111*, e24051.
[10] a) B. Bilgiçer, K. Kumar, *Proc. Natl. Acad. Sci. USA* **2004**, *101*, 15324–15329; b) N. Naarmann, B. Bilgiçer, H. Meng, K. Kumar, C. Steinem, *Angew. Chem. Int. Ed.* **2006**, *45*, 2588–2591.
[11] a) B. Meng, S. L. Grage, O. Babii, M. Takamiya, N. MacKinnon, T. Schober, I. Hutskalov, O. Nassar, S. Afonin, S. Koniev, I. V. Komarov, J. G. Korvink, U. Strähle, A. S. Ulrich, *Small* **2022**, e2107308; b) S. E. Kirberger, S. D. Maltseva, J. C. Manulik, S. A. Einstein, B. P. Weegman, M. Garwood, W. C. K. Pomerantz, *Angew. Chem. Int. Ed. Engl.* **2017**, *56*, 6440–6444; c) P. Wadhwani, P. Tremouilhac, E. Strandberg, S. Afonin, S. Grage, M. Ieronimo, M. Berditsch, A. S. Ulrich, in *Current Fluoroorganic Chemistry*, Vol. 949, American Chemical Society, **2007**, pp. 431–446.
[12] a) J. Leppkes, T. Hohmann, B. Koksch, *J. Fluorine Chem.* **2020**, *232*, 109453; b) T. Hohmann, M. Dyrks, S. Chowdhary, M. Weber, D. Nguyen, J. Moschner, B. Koksch, *J. Org. Chem.* **2022**, *87*, 10592–10604.
[13] S. Chowdhary, R. F. Schmidt, A. K. Sahoo, T. tom Dieck, T. Hohmann, B. Schade, K. Brademann-Jock, A. F. Thünemann, R. R. Netz, M. Gradzielski, B. Koksch, *Nanoscale* **2022**, *14*, 10176–10189.
[14] K. Ataka, T. Kottke, J. Heberle, *Angew. Chem. Int. Ed.* **2010**, *49*, 5416–5424.
[15] J. Leppkes, N. Dimos, B. Loll, T. Hohmann, M. Dyrks, A. Wieseke, B. G. Keller, B. Koksch, *RSC Chem. Biol.* **2022**, *3*, 773–782.
[16] M. Paradís-Bas, J. Tulla-Puche, F. Albericio, *Chem. Soc. Rev.* **2016**, *45*, 631–654.
[17] P. Wallimann, R. J. Kennedy, J. S. Miller, W. Shalongo, D. S. Kemp, *J. Am. Chem. Soc.* **2003**, *125*, 1203–1220.
[18] a) A. A. Adzhubei, M. J. E. Sternberg, A. A. Makarov, *J. Mol. Biol.* **2013**, *425*, 2100–2132; b) Z. Shi, K. Chen, Z. Liu, N. R. Kallenbach, *Chem. Rev.* **2006**, *106*, 1877–1897; c) Z. Shi, R. W. Woody, N. R. Kallenbach, in *Advances in Protein Chemistry*, Vol. 62, Academic Press, **2002**, pp. 163–240; d) B. Bochicchio, A. M. Tamburro, *Chirality* **2002**, *14*, 782–792.
[19] P. M. Cowan, S. McGavin, *Nature* **1955**, *176*, 501–503.
[20] a) F. Eker, K. Griebenow, R. Schweitzer-Stenner, *J. Am. Chem. Soc.* **2003**, *125*, 8178–8185; b) Z. Liu, K. Chen, A. Ng, Z. Shi, R. W. Woody, N. R. Kallenbach, *J. Am. Chem. Soc.* **2004**, *126*, 15141–15150.
[21] V. Kubyshkin, S. L. Grage, J. Bürck, A. S. Ulrich, N. Budisa, *J. Phys. Chem. Lett.* **2018**, *9*, 2170–2174.
[22] A. L. Rucker, T. P. Creamer, *Protein Sci.* **2002**, *11*, 980–985.
[23] A. I. Arunkumar, T. K. S. Kumar, C. Yu, *Biochim. Biophys. Acta (BBA) – Protein Structure and Molecular Enzymology* **1997**, *1338*, 69–76.
[24] V. Kubyshkin, J. Bürck, O. Babii, N. Budisa, A. S. Ulrich, *Phys. Chem. Chem. Phys.* **2021**, *23*, 26931–26939.
[25] J. L. S. Lopes, A. J. Miles, L. Whitmore, B. A. Wallace, *Protein Sci.* **2014**, *23*, 1765–1772.
[26] Z. Shi, C. A. Olson, D. Rose George, L. Baldwin Robert, R. Kallenbach Neville, *Proc. Nat. Acad. Sci.* **2002**, *99*, 9190–9195.
[27] K. Ataka, J. Drauschke, V. Stulberg, B. Koksch, J. Heberle, *Biochim. Biophys. Acta Biomembr.* **2022**, *1864*, 183873.
[28] K. Pagel, K. Seeger, B. Seiwert, A. Villa, A. E. Mark, S. Berger, B. Koksch, *Org. Biomol. Chem.* **2005**, *3*, 1189–1194.
[29] a) T. J. Measey, R. Schweitzer-Stenner, *J. Am. Chem. Soc.* **2006**, *128*, 13324–13325; b) R. Schweitzer-Stenner, T. Measey, A. Hagarman, F. Eker, K. Griebenow, *Biochemistry* **2006**, *45*, 2810–2819.
[30] D. J. Tew, S. P. Bottomley, D. P. Smith, G. D. Ciccotosto, J. Babon, M. G. Hinds, C. L. Masters, R. Cappai, K. J. Barnham, *Biophys. J.* **2008**, *94*, 2752–2766.
[31] J. M. Rausch, J. R. Marks, R. Rathinakumar, W. C. Wimley, *Biochemistry* **2007**, *46*, 12124–12139.
[32] Z. Lai, X. Yuan, H. Chen, Y. Zhu, N. Dong, A. Shan, *Biotechnol. Adv.* **2022**, *59*, 107962.
[33] a) S. Huhmann, B. Koksch, *Eur. J. Org. Chem.* **2018**, *2018*, 3667–3679; b) R. Smits, B. Koksch, *Curr. Top. Med. Chem.* **2006**, *6*, 1483–1498.
[34] L. Hedstrom, *Chem. Rev.* **2002**, *102*, 4501–4524.
[35] a) I. Schechter, A. Berger, *Biochem. Biophys. Res. Commun.* **1967**, *27*, 157–162; b) I. Schechter, A. Berger, *Biochem. Biophys. Res. Commun.* **1968**, *32*, 898–902.
[36] B. Koksch, N. Sewald, H.-J. Hofmann, K. Burger, H.-D. Jakubke, *J. Peptide Sci.* **1997**, *3*, 157–167.
[37] H. Meng, K. Kumar, *J. Am. Chem. Soc.* **2007**, *129*, 15615–15622.
[38] L. M. Gottler, R. de la Salud Bea, C. E. Shelburne, A. Ramamoorthy, E. N. G. Marsh, *Biochemistry* **2008**, *47*, 9243–9250.
[39] a) N. J. Harris, E. Reading, K. Ataka, L. Grzegorzewski, K. Charalambous, X. Liu, R. Schlesinger, J. Heberle, P. J. Booth, *Sci. Rep.* **2017**, *7*, 8021; b) A. Baumann, S. Kerruth, J. Fitter, G. Büldt, J. Heberle, R. Schlesinger, K. Ataka, *PLoS One* **2016**, *11*, e0151051; c) K. Ataka, S. T. Stripp, J. Heberle, *Biochim. Biophys. Acta Biomembr.* **2013**, *1828*, 2283–2293.

Manuscript received: December 9, 2022
Accepted manuscript online: February 1, 2023
Version of record online: March 15, 2023